Link sito dell'editore: https://www.journals.elsevier.com/composites-part-b-engineering

Link codice DOI: 10.1016/j.compositesb.2018.02.026

Citazione bibliografica dell'articolo:

F. Lionetto, C. Mele, P. Leo, S. D'Ostuni, F. Balle, A. Maffezzoli. *Ultrasonic spot welding of carbon fiber reinforced epoxy composites to aluminum: mechanical and electrochemical characterization.* Composites Part B, 144 (2018) 134-142

Ultrasonic spot welding of carbon fiber reinforced epoxy composites to aluminum: mechanical and electrochemical characterization

Francesca Lionetto[1]*, Claudio Mele[1], Paola Leo[1], Sonia D'Ostuni[1], Frank Balle[2], Alfonso Maffezzoli[1]

[1]*Department of Engineering for Innovation, University of Salento, via per Monteroni, 73100 Lecce, Italy*

[2]*Institute of Materials Science and Engineering, Hybrid Materials Engineering Group, University of Kaiserslautern, P.O. Box 3049,67653 Kaiserslautern, Germany*

**corresponding author email: francesca.lionetto@unisalento.it*

Abstract

The mechanical and electrochemical behavior of ultrasonic spot welded hybrid joints, made of AA5754 aluminum and carbon fiber reinforced epoxy with a co-cured thermoplastic surface layer, was studied. The effect of the welding parameters (energy and force) and the thickness of a thermoplastic film, applied as an upper ply in the composite lay-up, on the development of adhesion strength, was investigated. The best mechanical results were obtained when the welding parameters were able to achieve a large bonding area of mechanical interlocking between naked carbon fibers and aluminum and a better load distribution. The electrochemical results excluded the possibility of galvanic corrosion between aluminum and composite adherends thanks to the insulating action provided by the thermoplastic film.

Keywords: A. Polymer–matrix composites (PMCs); B. Mechanical properties, D. Ultrasonics; E. Joints/joining

Introduction

The increasing use of carbon fiber reinforced polymers (CFRP) in different fields and the emerging trend towards lightweight, high performance and high functionality components is leading to the use of multi-material hybrid structures. This involves the need for joining dissimilar materials, such as CFRPs and metals, which is a challenging task using conventional joining methods due to the different physical and chemical properties of the joining materials [1]. Ineffective joining procedures can drastically reduce the efficiency gained by the use of these structures [2]. The most frequently used joining methods for CFRP and metals are mechanical fastening and adhesive bonding. Conventional mechanical joining processes by means of bolts or rivets usually presents several disadvantages associated to the long joining time required by the hole-drilling and fastening operations and to the cut of the reinforced fibers [3]. This latter leads to a reduction of load carrying capability of the composite material due to stress concentrations and to delaminations and peeling through the plies of the composite [4], [5], [6], [7]. Some of these drawbacks have been overcome by recently developed fast joining processes such as clinching [8] and self-pierce riveting [9]-[10] which do not require preliminary drilling of a hole in the sheets [11]. However, although the delamination introduced by these mechanical joining processes is reduced compared to traditional mechanical fastening, this problem is

still under investigation. Furthermore, fasteners are exposed to corrosion and increase the weight of structures due to their additional mass [12],[13]. Adhesive bonding is an expensive method which requires a careful surface preparation before joining and a long curing time [14], [15]. The required adhesion properties are reached only if the crosslinking process is properly carried out in terms of time and temperature [16]. Other disadvantages of this technology are the low durability of adhesive joints and the harmful environmental emissions [17], [18]. In particular, the selection of proper adhesives is critical for joining dissimilar materials because the adhesive degradation with time can significantly reduce the bonding strength [19].

Suitable joining technologies are necessary in order to overcome the limitations related to convectional joining methods and the consequent loss of performance in the final assembly. Recently, different ~~welding~~ technologies and approaches for joining dissimilar materials have been developed. Examples include resistance welding [20], [21], [22], laser welding [13], [23], [24], [25], friction spot welding [26],[27], friction stir welding [28], [29], [30], [31] and induction welding [32], [15]. In all cases, thermoplastic matrix composites have been joined to metals, since thermoset matrices do not melt due to their crosslinked structure.

Among welding processes available to industry, ultrasonic welding is an attractive solution for joining light materials through the simultaneous application of localized high-frequency (20-40 kHz) vibratory energy and clamping forces [33], [34], [35], [36], [37], [38], [39]. Ultrasonic ~~spot~~ welding presents several advantages over conventional welding and adhesive bonding such as very short welding times, highly localized heating, low energy input and ease of automation. Very recently, some of the authors demonstrated the feasibility of hybrid ultrasonic ~~spot~~ welding of carbon fiber reinforced epoxy to AA5754 aluminum by using a semi-crystalline thermoplastic film of polyamide 6 (PA6) co-cured as a surface layer of the composite stack [40]. During ultrasonic welding, the local fast increase in the temperature leads to melting of PA 6 layer, which is displaced out of the welding zone underneath the sonotrode by the pressure applied by the sonotrode. At the same time, the metallic sheet is plastically deformed and a direct contact between aluminum surface and carbon fibers is realized. The approach of modifying the surface of a thermosetting matrix composite by using a co-cured thermoplastic film has been proved to be successful also in the case of welding of two thermosetting matrix composite adherends, as recently demonstrated by Lionetto et al. [41].

Despite the preliminary good mechanical performance of hybrid CF/epoxy-AA5754 joints, a systematic investigation on the role of the thermoplastic film and welding parameters on the bonding mechanisms and mechanical performance is still lacking. Moreover, the high electrical conductivity of carbon fibers can generate a galvanic cell in the presence of an electrolyte or conductive ionic solution. Since carbon fibers are very efficient cathode and very noble in the galvanic series, the electrical contact between CFRPs and metals with similar properties in presence of water which contains electrolytes can lead to the corrosion of metal [42], [43], [44]. Although the danger of galvanic corrosion was generally recognized, little work is available to quantitatively measure the extent of corrosion of hybrid metal-composite joints. The possibility and intensity of galvanic corrosion between CFRPs and aluminum was recently studied in mechanically fastened

and bonded structures [42],[45], [10], [46], [47]. To the author knowledge, there is no work in the literature on the evaluation of corrosion behavior of welded CFRP-aluminum joints.

~~In this paper, the mechanical and electrochemical behavior of ultrasonic spot welded thermosetting composite-aluminum joints has been presented.~~ This paper is focused on the mechanical and electrochemical characterization of ultrasonic spot welded hybrid joints, made of AA5754 aluminum and carbon fiber reinforced epoxy, joined with a novel method recently developed by the authors using ultrasonic spot welding and a co-cured thermoplastic surface layer. Compared to the paper recently published by the same authors (ref 32, now [40]), which presented preliminary results showing the potential of the joining method, the novelty of this work is based on i) a study of the adhesion mechanism between the two dissimilar joining partners through a morphological analysis; ii) an analysis of the effect of interlayer thickness on the adhesion mechanism and mechanical performance; iii) an electrochemical study of the welded joint, which has never been carried on welded CFRP-aluminum joints. Both potentiostatic and potentiodynamic polarization and zero resistance ammeter (ZRA) measurements have been used to evaluate the corrosion behavior and the eventual insulating action of the thermoplastic interlayer film.

~~The effect of both the welding parameters and the thickness of the thermoplastic interlayer film on the development of adhesion strength have has been analyzed and discussed. The adhesion mechanism between the adherends has been studied by optical microscopy of fracture surfaces and cross sections of the welded joints. Moreover, Finally, an electrochemical study of the welded CFRP-aluminum joint has been performed for the first time the evaluation of to evaluate its corrosion behavior. of welded CFRP-aluminum joints.~~

~~the possibility of galvanic corrosion between aluminum and CFRP adherends in welded hybrid joints has been also studied.~~

~~Experimental~~ Materials and Methods

Constituent materials of the hybrid joints

The composite adherend of the hybrid joint was a carbon fiber reinforced epoxy laminate widely used in the automotive and aeronautical industry. It was prepared using a carbon fiber-epoxy prepreg,TC-EP250TU2-1 supplied by Technologycom S.r.l. (Italy).The prepreg matrix was a toughened epoxy resin, based on a diglycidyl ether of bisphenol A (DGEBA) resin. The prepreg reinforcement was a high strength carbon fabric (twill 2/2,55 % by volume). A Polyamide 6 (PA6) film (Wrightlon® 7400, Airtech Europe Sarl) was used to promote the adhesion of hybrid metal-composite joint. The used films had three different thicknesses: 50, 100 and 150 μm. The thermal properties of the thermoplastic film have been previously investigated [40]. The composite adherends used for the ultrasonic welding process were cut from plate-shaped laminates (300 x 200 x 2 mm^3). These latter were manufactured by vacuum bagging of 9 plies of CF/epoxy prepregs which were stacked adding the PA6 film as a last ply. After composite curing for one hour at 125 °C under vacuum and cooling down to room temperature, composite strips of 70 x 30 x 2 mm^3size were cut.

The metallic adherend of the hybrid joint was AA5754 Aluminum alloy, based on Al-Mg system, characterized by good formability, high fatigue strength, corrosion resistance and fair machinability. This alloy is often used in the automotive industry for structural parts and inner body panels[48]. The dominant strengthening mechanisms are work hardening and solute strengthening. In fact, for Al-Mg alloys the hardening coming from second phases particles (aging heat treatment) is very low in comparison with solution hardening or work hardening [48], [49]. Homogenization treatments lead to dissolution of soluble particles (for example Mg_2Si) so increasing the hardness by solid solution strengthening [50], [51], [52]. The aluminum sheets (70 x 25 x 1 mm^3) were only cleaned by ethanol and welded in an as-rolled condition without any further surface pre-treatment. In Figure 1 is reported a sketch (not in scale) of the hybrid joint analyzed in this work.

Ultrasonic spot welding

The ultrasonic welding system was M4000 supplied by Telsonic Ultrasonics AG, shown in Figure 2. The system was able to control the ultrasonic force, the ultrasonic energy and the amplitude of oscillation of the sonotrode. The ultrasonic welding setup was characterized by a clamping system for both the upper and the lower joining partner. ~~After loading both the metal and the composite partner into the ultrasonic welder setup (Figure 2a), the sonotrode was lowered until its square tip exerts a given pressure while sending the ultrasonic waves to the adherends (Figure 2b). At the end of the welding process, the sonotrode was raised (Figure 2c). An example of CF/epoxy-PA6-AA5754 joint after ultrasonic welding is reported in Figure 2d.~~ The AA5754 and CF/epoxy sheets were fixed in the clamping jig (Figure 2a). The sonotrode was lowered until its square tip exerted a given welding force (F_{US}) while sending the ultrasonic oscillations (u) via the upper joining partner to the hybrid interface (Figure 2b). At the end of the welding process, the sonotrode was raised (Figure 2c). An example of one ultrasonically welded hybrid joint with its final geometry and the characteristic imprint of the sonotrode tip, whose area is 10 x 10 mm^2, is shown in Figure 2d. In this study, ultrasonic energy between 2160 J and 2500 J and force between 140 N and 320 N were used.

Characterization

The adhesion strength was evaluated by tensile lap-shear tests carried out according to the DIN EN 1465 standard. A Schenk dynamometer with a crosshead speed of 2 mm/min and a maximum force of 25 kN was used. For comparison purposes, lap shear tests were performed also on CF/epoxy-PA6-CF/epoxy joints and AA5754-PA6-AA5754 joints. These joints were obtained by adhesive bonding in oven at 230 °C using PA6 as the adhesive. At least eight replicates for each condition were analyzed. Morphological characterization of cross-sections was carried out by means of Nikon Ephipot 200 optical microscope. The morphology of the fractured samples was examined by Nikon stereomicroscope PL 1000 and by scanning electron microscopy (SEM) with Energy-Dispersive X-ray Spectroscopy (EDS) analysis using a Zeiss EVO 40 instrument operating with a voltage of 20 kV.

Electrochemical measurements were performed with a PARSTAT 2273 potentiostat/galvanostat in an aqueous 3.5% NaCl solution. All experiments were conducted in naturally aerated, near neutral solutions at

ambient temperature. A conventional three-electrode cell was employed, with a platinised titanium expanded mesh counter electrode, a Ag/AgCl reference electrode and a specimen of AA5754aluminium, of CF/epoxy or of the welded hybrid joint as a working electrode. All the potentials were referred to Ag/AgCl. The samples were insulated using teflon to mask their cut edges and back sides, in order to leave only a surface area of 1 cm^2exposed to the electrolyte. The steady state potential was determined after 30 minutes of immersion in the solution at open circuit potential (OCP). Following the determination of the steady state OCP, potentiodynamic polarisation measurements were performed from -1.3 V to 0 V at a scan rate of 1 mV s^{-1}. Galvanic coupling studies were carried out by coupling one by one, aluminium, CF-epoxy and hybrid welded joint specimens with an aluminium reference sample. During the test, the coupling current densities and the mixed potential of the coupled electrodes were monitored for 20 hours by means of a zero-resistance ammeter (ZRA), using a Ag/AgCl reference electrode. Table 1 reports the analysed joint typologies and the relative experimental characterization.

~~Mechanical results~~ Results and Discussion

Effect of welding energy and welding force on adhesion strength

The effect of the welding energy and welding force on the adhesion strength of hybrid Al/CF-epoxy joints has been evaluated by means of monotonic lap shear tests. The lap shear strength (LSS) of hybrid joints realized with a PA6 film of 100 µm thickness is reported in Figure 3. A significant increase in the average LSS from 22.7 ± 3.7 MPa to 34.8 ± 3.9 MPa is observed when the welding energy is increased from 2160 J to 2300 J, respectively. Intermediate values of welding energy (2300 J) produce the strongest joint. ~~while the~~ The highest welding energy (2500 J) produce joints with slightly reduced mechanical performance (33.2 ± 3.9 MPa) even if the difference of LSS at 2300 J and 2500J is not statistically relevant.

A second set of experiments has been carried out for ultrasonically welded hybrid joints with ~~the energy that gives the best performance (2300 J)~~ an energy of 2300 J and different welding forces, ranging from 140 N to 320 N. The lowest sonotrode force (140 N) does not provide adequate connection to the hybrid adherends. An increase of joint strength with welding force is observed in Figure 3b, where significant effects on the quality of the joints can be obtained by using a welding force of 280 N or higher.

The observation of fracture surfaces of hybrid joints has enabled to understand the effect of welding parameters on the bonding mechanism. As reported in Figure 4 a-b, the fracture surfaces of the hybrid joints welded at 2160 J are characterized by at least two different zones. The first inner zone, marked by white dashed line and labeled as I, indicates the zone underneath the sonotrode tip, where carbon fibers are directly bonded to aluminum. Mechanical interlocking due to plastic deformation of the aluminum at the interface to carbon fibers is the dominant bonding mechanism in this zone. The second zone, marked by a black dashed line and labelled as “A”, is characterized by the adhesion of PA6 to the adherends since it is clearly visible the presence of a very thin layer of PA6 covering both the metal and composite sheets. PA6-rich zones remain attached to the adherends, as evidenced by the arrows (Figures 4a-b). As can be inferred by Figure 4 a-b, the A area is larger than I area. The prevalence of an adhesive bonding instead of a mechanical

interlocking of the adherend surfaces is responsible of the low mechanical response of the joint welded using the lowest energy. In fact, the adhesion of PA6 to metal or composite substrate has been experimentally evaluated by means of single lap tests carried out on CF/epoxy-PA6-CF/epoxy joints and AA5754-PA6-AA5754 joints. These joints were adhesively bonded in oven at 230°C using PA6 as the adhesive. They were realized with the aim to estimate the contribution to the overall single lap shear strength given by the adhesion of PA6 to aluminum and to CF/epoxy. An average adhesion strength of 3.88 ± 0.33 MPa and 3.14 ± 0.30 MPa were found for CF/epoxy-PA6-CF/epoxy joints and AA5754-PA6-AA5754 joints, respectively.

The fracture surfaces of the hybrid joints welded at 2300 J (Figure 4c-d) are characterized by the presence of a wide "I-zone" where carbon fibers are directly connected to the aluminum surface, evidenced by the white dashed line. The value of this area (100 ± 2 mm^2) corresponds to the nominal area of the sonotrode tip. This indicates that a proper combination of welding parameters (2300 J and 280 N) leads to a complete squeeze-out of the PA6 film from the sonotrode contact area and promotes the formation of a quite homogenous micromechanical interlocking between carbon fibers and aluminum. It can be concluded that, this interlocking provides the dominant contribution to mechanical performances of the studied ultrasonically welded hybrid joints. Outside the mechanical interlocking area, an adhesion area is still present, where thin layers of PA6 are mostly found attached to the CF/epoxy surface and partially to aluminum surface. On the aluminum side of the fracture surfaces of the examined samples (Figure 4c) it is possible to observe the imprints of carbon fibers in the "I-zone".

By increasing the welding energy to 2500 J, a further increase of the I-zone characterized by mechanical interlocking is observed in Figure 4e-f. Its value, calculated by digital image analysis is 108 ±3 mm^2. By using this value for the calculation of strength, slightly lower LSS values than those obtained at 2300 J were found. The larger I-zone can be associated to the higher frictional heat generated at 2500 J, which fast decreases the viscosity of the molten PA6. Thus, a larger amount of the molten PA6 is squeezed out of the bonding area. A larger amount of squeezed molten PA6 polymer for the high energy samples compared to low energy sample is observable in Figure 4 e-f. The adhesion zone is still present and the PA6 rich zones are characterized by a yellowish color indicating the initial thermal degradation in the PA6 due to the high temperature reached during welding. On the aluminum side of the fracture surfaces of the examined samples (Figure 4e) it is possible to observe the imprints of carbon fibers in the I-zone. This is the result of a mechanical interlocking at the interface, which mainly contributes to the strength of the joints.

The presence of carbon fiber imprints on the aluminum fracture surface has been confirmed by scanning electron microscopy (SEM) with EDS analysis. In Figure 5 a magnified SEM micrograph of the bonded I-zone of the aluminum fracture surface reported in Figure 4 c is shown. The black traces (Figure 5 a, d) can be attributed to carbon fibers which remain on the Al fracture surface after ultrasonic spot welding due to a strong bond and cohesive failure of the composite surface plies. In particular, an EDS mapping of these areas (Figures 5e and 5f) points up the presence of carbon, defined by green color, and present in the same position of the darkest areas of Figure 5d.

The mechanism of bond formation during ultrasonic welding can be inferred from the obtained results. The welding process for Al/CFRP-joints is very fast with a duration between 2.5 s and 3.5 s depending on the welding energy. The initial stage of the ultrasonic metal welding, when the metal adherend moves relatively to the composite adherend, is governed by dry friction and viscoelastic heating. The strong relative motion of the aluminum sheet at the interface with the CF/epoxy-PA6 sheet is responsible for an abrasive wear of the surface asperities which produces a very fast increase in temperature underneath the sonotrode tip. As temperature increases, viscous losses became the main heating source until PA6 melts. This leads to an initial degradation of the epoxy matrix of the first composite ply. Due to the ~~longitudinal~~ ultrasonic oscillations and the pressure applied by the sonotrode, the molten PA6 polymer is displaced out from the contact area underneath the sonotrode tip and squeezed out to the edges of the aluminum sheet into a region where only some weak adhesion between PA6 and aluminum could occur. At the same time, the application of high pressure and high frequency shear oscillations at an increasing temperature (with a maximum between 300 and 400 °C depending on the welding energy [34]) causes a pronounced plastic deformation of the aluminum surface at the interface to the stiffer carbon fibers. A direct contact between carbon fibers and aluminum enables a strong bond, especially due to mechanical interlocking and direct connection between fibers and aluminum. The PA6 interlayer is therefore necessary for obtaining the joining of composite and metal adherend. Without this interlayer film, the hybrid joining is not possible. In fact, the same ultrasonic spot welding experiments carried out on CF epoxy and aluminum adherends without the PA6 interlayer does not give any adhesion of the two adherends.

The welding energy greatly affects the quality of the interfacial zone. Since the oscillation amplitude used in this study has been kept constant at 40 µm, the different welding energies involve different welding times. By using the lowest energy value of 2160 J, the welding time is probably too short to enable a sufficient melting and squeezing of the thermoplastic interlayer film and the removal of the surface micrometric layers of epoxy resin of the first composite ply. Therefore, a small residual PA6 layer is left in between aluminum surface and CF/epoxy composite sheet. This is confirmed by the optical microscopy of cross-sections of hybrid joints welded with an energy of 2160 J and an oscillation amplitude of 40 µm (Figure 6a).

On the other hand, the use of the highest welding energy (2500 J) probably leads to an excessive heat input and some damage on the adherends, as evidenced by charred epoxy, damaged carbon fibers and detached aluminum debris observable in Figure 6c. In fact, the removal of the epoxy resin of the underlying plies, reduced the mechanical properties of the composite adherend and, consequently, of the entire hybrid Al/CFRP joint. These defects are similar to those reported by Lambiase et al. [53] for laser-assisted direct-joining of carbon fiber reinforced epoxy to polycarbonate sheets.

The best mechanical results were obtained for welding parameters (energy and force) leading to a larger area of mechanical interlocking between carbon fibers and aluminum as well as to a better load distribution without an excessive matrix degradation. The cross-section of a such hybrid joint reported in Figure 6b confirms the direct contact between carbon fibers and aluminum with a homogenous interface.

The temperature, measured during ultrasonic spot welding by a K-type thermocouple positioned between aluminium and composite adherend, is in the range 350-400 °C depending on the welding parameters. A similar range has been also measured by an infrared camera. From TGA analysis, here not reported, the onset of epoxy degradation, calculated as the temperature at which 5% weight loss is observed, is equal to 375 °C at a heating rate of 10 °C/min. At the extremely high heating rates during ultrasonic welding process, the onset of epoxy degradation is expected to occur at higher temperatures than 375 °C. Considering also that these high temperatures are experimented by the composite only for fractions of second, it is reasonable to think that only the degradation of the surface epoxy layer of composite partner occurs.

Effect of ultrasonic welding force and PA6 thickness on adhesion strength

The results previously analyzed indicate that the PA6 film co-cured in the composite laminate has an active role in the bonding mechanism during ultrasonic spot welding. This suggests that the thickness of the PA6 film can significantly affect the joint quality. In order to verify this hypothesis, the effect of the thickness of the PA6 film on the lap shear strength of hybrid Al/CFRP-joints was evaluated by lap shear test under tensile loading. The lap shear strength of hybrid joints with a PA6 film thickness of 50, 100 and 150 μm, welded at three different welding forces, is reported in Figure 7.

The hybrid joints prepared with a PA6 film thickness of 50 μm are characterized by the worst mechanical performances. The values of lap shear strength (LSS) are in the range between 23.1 ± 3.0 MPa and 26.2 ± 3.1 MPa, being significantly lower than those obtained in the hybrid joints with higher PA6 thickness. Moreover, the LSS values seem to be not significantly affected by the welding force. When the thickness of the PA6 film is increased to 100 μm, the corresponding hybrid joint presents superior lap shear strength of about 10%, 33% and 23% at a welding force of 180, 280 and 320 N, respectively. The hybrid joints prepared with a PA6 film thickness of 150 μm present LSS values not significantly different from those obtained using a PA6 film of 100 μm.

Figure 8 shows the representative fracture surfaces of the hybrid joints with different PA6 film thickness. The fracture surface on the CF/epoxy side (Figure 8a) shows an irregular aspect, characterized by the presence of several wrinkled and broken carbon fiber bundles. The bonding area is evidenced in Figure 8a by a dashed line. No traces of residual PA6 can be observed in the bonding area. The measured bonding area is 102 ± 5 mm^2, which corresponds to the sonotrode tip area. The mechanical results of Figure 7 and the fracture surfaces of Figure 8a suggest that the optimal thickness for obtaining a high adhesion strength is correlated with the energy input and its duration provided by ultrasonic spot welding. In case of a too thin thermoplastic PA6 film, the simultaneous action of ultrasonic oscillation and sonotrode pressure damages the surface of CF/epoxy laminate by breaking and wrinkling the carbon fibers due to excessive friction and shearing after PA6 melting and squeezing out from the welding area. This prevents the formation of a strong mechanical interlocking between carbon fibers and aluminum.

As observable in Figure 8b,the composite fracture surface of the joint with 100 ~~mm~~ μm PA6 interlayer is free of PA6 or epoxy traces indicating a direct contact between carbon fibers and aluminum. This suggests

the formation of a homogeneously distributed mechanical interlocking between composite and aluminum adherents. This enables a better and homogenous load transfer between the two adherends, thus improving the joint quality. The overall bonding area (105 ± 5 mm^2) is higher than that measured in the joint with 150 ~~mm~~ µm PA6 interlayer, which is 94 ± 4 mm^2. As reported in Figure 8c, the welding area is characterized by the presence of single molten and recrystallised PA6 spots, as evidenced by arrows. The reduced area of direct contact between carbon fibers and aluminum is responsible of the slightly decreased mechanical performance of the corresponding hybrid joints.

Electrochemical behavior

Figure 9a~~10a~~ shows the change of OCP of aluminum, CFRP and welded hybrid joint specimens in the near-neutral aqueous 3.5% NaCl solution, monitored for 30 minutes. As expected, the OCP value for the investigated AA5754 is about -0.77 V vs. Ag/AgCl [54], [55]. It is also evident that the OCP value mainly increases during the first 10 minutes of immersion until reaching a constant potential, probably due to the coarsening of the oxide film. The CFRP specimen has an OCP value of about +0.15 V, resulting more noble than the investigated aluminum alloy, indicating that this latter is more susceptible to corrosion attack under similar conditions. The OCP value measured for the welded hybrid joint results substantially comparable with that of aluminum, presumably due to the effectiveness of spot welding, that leads to the exposure only of aluminum to the aggressive solution.

According to the literature, the galvanic corrosion behavior of the joint materials can be evaluated by an analysis of the potentiodynamic polarization curves of the single tested components[56], [10] and by ZRA galvanic corrosion tests. In fact, during the joining process, an electric contact between the carbon fibers of the CFRP and the aluminum sample was achieved. The potentiodynamic polarization behavior of the samples of aluminum, CFRP and welded joint specimens is reported in Figure ~~10b~~ 9b. From the polarization curves, the values of corrosion potential (E_{corr}), corrosion current density (i_{corr}) and pitting potential (E_{pit}) have been extracted and summarized in Table ~~1~~ 2. The polarization curve of the aluminum alloy reveals a passive region followed by a transpassive region. The two regions are divided by E_{pit}, which is equal to -0.68 V. Polarization of aluminum shows much higher i_{corr}, with respect to CFRP, indicating a higher susceptibility of AA5754 to corrosion in the aggressive solution containing chloride ions. Moreover, E_{corr} of aluminum results much lower than that of composite, confirming that aluminum will be anodic with respect to CFRP if they are galvanically coupled. E_{corr}, E_{pit} and i_{corr} extracted from the polarization curve of the welded joint resulted comparable to the corresponding values obtained for AA5754. This indicates that the ultrasonic spot welding performed in this study leads to the exposition only of aluminum to the solution thus not allowing the electrolyte to penetrate at the interface between aluminum and CFRP.

The coupling behavior between aluminum alloy and CFRP has been investigated also by ZRA galvanic corrosion tests. The galvanic current density (i_{galv}) and galvanic corrosion potential (mixed potential, E_{mixed}) were measured over an immersion period of 20 hours in 3.5% NaCl solution. i_{galv} and E_{mixed} of CFRP and of welded joint resulting from a separately coupling with a reference aluminum specimen are presented in

Figure ~~11a~~ 10a and ~~11b~~ 10b respectively. The experimental plot of galvanic coupling of aluminum with the aluminum reference sample is also reported for comparison. i_{galv} measured by coupling CFRP and aluminum is almost constant with an average value of 175 ± 5 μA cm^{-2} during the 20 hours of the test, showing a high level of galvanic corrosion sensitivity [47]. Moreover, the slight decrease of i_{galv} with time can be ascribed to the increase of the corrosion products that protect the aluminum substrate. The inhibition effect of corrosion products was already observed in the literature on steel, magnesium and aluminum alloys [57], [45], [42], [43]. The average i_{galv} measured by coupling the welded joint and the aluminum sample with a AA5754 reference specimen during the 20 hours of the test are -0.39 ± 2.62 μA cm^{-2} and 1.00 ± 2.26 μA cm^{-2}, respectively.

The electrochemical results demonstrate that, although a direct electric contact between the carbon fiber composite and aluminum, no evident effect of galvanic corrosion can be observed in the welded hybrid joint immersed in the chloride solution. This indicates that in the proposed welding approach the thermoplastic PA6 film acts as a skirting medium that isolates the CFRP and aluminum adherends, thus protecting from corrosion the welded area.

Conclusions

~~In this work~~ ultrasonic metal welding was applied to join AA5754 aluminum sheets to a thermoset matrix composite consisting of a carbon fiber reinforced epoxy resin with the top surface modified by the presence of a co-cured polyamide 6 layer. From the mechanical, morphological and electrochemical characterization, the following conclusions can be drawn:

1) During ultrasonic spot welding, the strong friction between the aluminum sheet and the CF/epoxy-PA6 sheet ~~is responsible for an abrasive wear of the surface asperities which~~ produces a very fast increase in temperature underneath the sonotrode tip. This leads to PA6 melting and to a limited degradation of the epoxy matrix of the first composite ply~~. Due to the longitudinal oscillations and the pressure applied by the sonotrode, the molten PA6 polymer is displaced out from the contact area under the sonotrode tip and squeezed out to the edges of the aluminum sheet into a region where only some weak adhesion between PA6 and aluminum could eventually occur~~. ~~At the same time,~~ The application of high force and high frequency shear oscillations at an increasing temperature causes both the squeezing of molten PA6 polymer out from the contact area under the sonotrode tip and a pronounced plastic deformation in the aluminum adherend. A direct contact between carbon fibers and aluminum is thus formed which enables a high adhesion due to mechanical interlocking.

2) The welding energy and force have a strong effect in providing mechanical interlocking at microscopic level. At a constant oscillation amplitude, welding energy affects the temperature increase in the welding area, which should be sufficient to completely melt the PA6 film without an excessive epoxy matrix degradation. On the other hand, the welding force is important for squeezing the molten PA6 matrix out from the welding area. ~~The highest adhesion strength (34.8 MPa) was obtained using welding energy and force~~

~~(2300 J and 280 N) thanks to a large bonding area where mechanical interlocking between carbon fibers and aluminum is the dominant adhesion mechanism.~~

3) The PA6 film plays an active role in promoting the adhesion without damaging the carbon fibers. A film thickness of 100 μm is the most appropriate to obtain hybrid joints characterized by a high single lap shear strength.

4) Electrochemical tests demonstrated that, in the studied ultrasonic spot welded CF/epoxy-AA5754 joints, galvanic corrosion is prevented by the presence of the thermoplastic PA6 film, which acts as an electrical insulation layer that prevents the direct contact of the water solution with the area where carbon fibers and aluminum are in contact, thus protecting from corrosion the welded area.

Acknowledgements

Francesca Lionetto acknowledges Deutscher Akademischer Austauschdienst (DAAD) for a grant for a Research Stays at the Institute of Materials Science and Engineering, University of Kaiserslautern. Mrs. Tiziana De Giorgi is kindly acknowledged for preparing the specimens. Dr. Daniel Backe, Mr Michael Becker and Mr Florian Staab are also acknowledged for their assistance during the ultrasonic welding experiments. Mr Donato Cannoletta is acknowledged for the SEM analysis.

References

[1] Martinsen K, Hu SJ, Carlson BE. Joining of dissimilar materials. CIRP Annals-Manufacturing Technology 2015;64:679–99.

[2] Studer J, Dransfeld C, Masania K. An analytical model for B-stage joining and co-curing of carbon fibre epoxy composites. Composites Part A: Applied Science and Manufacturing 2016;87:282–9.

[3] Lionetto F, Pappadà S, Buccoliero G, Maffezzoli A. Finite element modeling of continuous induction welding of thermoplastic matrix composites. Materials & Design 2017;120:212–21.

[4] Davim JP, Reis P, Antonio CC. Experimental study of drilling glass fiber reinforced plastics (GFRP) manufactured by hand lay-up. Composites Science and Technology 2004;64:289–97.

[5] Zitoune R, Collombet F. Numerical prediction of the thrust force responsible of delamination during the drilling of the long-fibre composite structures. Composites Part A: Applied Science and Manufacturing 2007;38:858–66.

[6] Parkes PN, Butler R, Meyer J, de Oliveira A. Static strength of metal-composite joints with penetrative reinforcement. Composite Structures 2014;118:250–6.

[7] Kabche J-P, Caccese V, Berube KA, Bragg R. Experimental characterization of hybrid composite-to-metal bolted joints under flexural loading. Composites Part B: Engineering 2007;38:66–78.

[8] Chen C, Zhao S, Cui M, Han X, Fan S. Mechanical properties of the two-steps clinched joint with a clinch-rivet. Journal of Materials Processing Technology 2016;237:361–70.

[9] Zhang X, He X, Xing B, Zhao L, Lu Y, Gu F, et al. Influence of heat treatment on fatigue

performances for self-piercing riveting similar and dissimilar titanium, aluminium and copper alloys. Materials & Design 2016;97:108–17.

[10] Mandel M, Krüger L. Electrochemical corrosion studies and pitting corrosion sensitivity of a self-pierce rivet joint of carbon fibre reinforced polymer (CFRP)–laminate and EN AW-6060-T6. Materialwissenschaft Und Werkstofftechnik 2012;43:302–9.

[11] Lambiase F, Ko D-C. Two-steps clinching of aluminum and carbon fiber reinforced polymer sheets. Composite Structures 2017;164:180–8.

[12] Ucsnik S, Scheerer M, Zaremba S, Pahr DH. Experimental investigation of a novel hybrid metal–composite joining technology. Composites Part A: Applied Science and Manufacturing 2010;41:369–74.

[13] Tan X, Zhang J, Shan J, Yang S, Ren J. Characteristics and formation mechanism of porosities in CFRP during laser joining of CFRP and steel. Composites Part B: Engineering 2015;70:35–43.

[14] Huang Z, Sugiyama S, Yanagimoto J. Hybrid joining process for carbon fiber reinforced thermosetting plastic and metallic thin sheets by chemical bonding and plastic deformation. Journal of Materials Processing Technology 2013;213:1864–74.

[15] Farahani RD, Dubé M. Novel Heating Elements for Induction Welding of Carbon Fiber/Polyphenylene Sulfide Thermoplastic Composites. Advanced Engineering Materials n.d.

[16] Lionetto F, Moscatello A, Maffezzoli A. Effect of binder powders added to carbon fiber reinforcements on the chemoreology of an epoxy resin for composites. Composites Part B: Engineering 2017;112:243–50.

[17] Arenas JM, Alía C, Narbón JJ, Ocaña R, González C. Considerations for the industrial application of structural adhesive joints in the aluminium–composite material bonding. Composites Part B: Engineering 2013;44:417–23.

[18] Lambiase F, Durante M, Di Ilio A. Fast joining of aluminum sheets with Glass Fiber Reinforced Polymer (GFRP) by mechanical clinching. Journal of Materials Processing Technology 2016;236:241–51.

[19] Pramanik A, Basak AK, Dong Y, Sarker PK, Uddin MS, Littlefair G, et al. Joining of carbon fibre reinforced polymer (CFRP) composites and aluminium alloys-A review. Composites Part A: Applied Science and Manufacturing 2017.

[20] Ageorges C, Ye L. Resistance welding of thermosetting composite/thermoplastic composite joints. Composites Part A: Applied Science and Manufacturing 2001;32:1603–12.

[21] Dubé M, Hubert P, Yousefpour A, Denault J. Resistance welding of thermoplastic composites skin/stringer joints. Composites Part A: Applied Science and Manufacturing 2007;38:2541–52.

[22] Stavrov D, Bersee HEN. Resistance welding of thermoplastic composites-an overview. Composites Part A: Applied Science and Manufacturing 2005;36:39–54.

[23] Kashaev N, Ventzke V, Riekehr S, Dorn F, Horstmann M. Assessment of alternative joining techniques for Ti–6Al–4V/CFRP hybrid joints regarding tensile and fatigue strength. Materials &

Design 2015;81:73–81.

[24] Chen YJ, Yue TM, Guo ZN. A new laser joining technology for direct-bonding of metals and plastics. Materials & Design 2016;110:775–81.

[25] Lambiase F, Genna S. Laser-assisted direct joining of AISI304 stainless steel with polycarbonate sheets: thermal analysis, mechanical characterization, and bonds morphology. Optics & Laser Technology 2017;88:205–14.

[26] André NM, Goushegir SM, dos Santos JF, Canto LB, Amancio-Filho ST. Friction Spot Joining of aluminum alloy 2024-T3 and carbon-fiber-reinforced poly (phenylene sulfide) laminate with additional PPS film interlayer: Microstructure, mechanical strength and failure mechanisms. Composites Part B: Engineering 2016;94:197–208.

[27] Goushegir SM, Dos Santos JF, Amancio-Filho ST. Friction spot joining of aluminum AA2024/carbon-fiber reinforced poly (phenylene sulfide) composite single lap joints: microstructure and mechanical performance. Materials & Design 2014;54:196–206.

[28] Singh R, Kumar R, Feo L, Fraternali F. Friction welding of dissimilar plastic/polymer materials with metal powder reinforcement for engineering applications. Composites Part B: Engineering 2016;101:77–86.

[29] Singh R, Kumar V, Feo L, Fraternali F. Experimental investigations for mechanical and metallurgical properties of friction stir welded recycled dissimilar polymer materials with metal powder reinforcement. Composites Part B: Engineering 2016;103:90–7.

[30] Nagatsuka K, Yoshida S, Tsuchiya A, Nakata K. Direct joining of carbon-fiber–reinforced plastic to an aluminum alloy using friction lap joining. Composites Part B: Engineering 2015;73:82–8.

[31] Adamus K, Adamus J, Lacki J. Ultrasonic testing of thin walled components made of aluminum based laminates. Composite Structures 2017.

[32] Mitschang P, Velthuis R, Didi M. Induction spot welding of metal/CFRPC hybrid joints. Advanced Engineering Materials 2013;15:804–13.

[33] Balle F, Wagner G, Eifler D. Ultrasonic metal welding of aluminium sheets to carbon fibre reinforced thermoplastic composites. Advanced Engineering Materials 2009;11:35–9.

[34] Wagner G, Balle F, Eifler D. Ultrasonic Welding of Hybrid Joints. JOM 2012;64:401–6.

[35] Wagner G, Balle F, Eifler D. Ultrasonic Welding of Aluminum Alloys to Fiber Reinforced Polymers. Advanced Engineering Materials 2013;15:792–803.

[36] Haddadi F, Abu-Farha F. Microstructural and mechanical performance of aluminium to steel high power ultrasonic spot welding. Journal of Materials Processing Technology 2015;225:262–74.

[37] Haddadi F, Tsivoulas D. Grain structure, texture and mechanical property evolution of automotive aluminium sheet during high power ultrasonic welding. Materials Characterization 2016;118:340–51.

[38] Lionetto F, Dell'Anna R, Montagna F, Maffezzoli A. Modeling of continuous ultrasonic impregnation and consolidation of thermoplastic matrix composites. Composites Part A: Applied Science and Manufacturing 2016;82:119–29.

[39] Lionetto F, Maffezzoli A, Ottenhof MA, Farhat I a., Mitchell JR. Ultrasonic investigation of wheat starch retrogradation. Journal of Food Engineering 2006;75:258–66.

[40] Lionetto F, Balle F, Maffezzoli A. Hybrid ultrasonic spot welding of aluminum to carbon fiber reinforced epoxy composites. Journal of Materials Processing Technology 2017;247.

[41] Lionetto F, Morillas MN, Pappadà S, Buccoliero G, Villegas IF, Maffezzoli A. Hybrid welding of carbon-fiber reinforced epoxy based composites. Composites Part A: Applied Science and Manufacturing 2018;104:32–40.

[42] Ireland R, Arronche L, La Saponara V. Electrochemical investigation of galvanic corrosion between aluminum 7075 and glass fiber/epoxy composites modified with carbon nanotubes. Composites Part B: Engineering 2012;43:183–94.

[43] Peng Z, Nie X. Galvanic corrosion property of contacts between carbon fiber cloth materials and typical metal alloys in an aggressive environment. Surface and Coatings Technology 2013;215:85–9.

[44] Arronche L, Gordon K, Ryu D, La Saponara V, Cheng L. Investigation of galvanic corrosion between AISI 1018 carbon steel and CFRPs modified with multi-walled carbon nanotubes. Journal of Materials Science 2013;48:1315–23.

[45] Liu Z, Curioni M, Jamshidi P, Walker A, Prengnell P, Thompson GE, et al. Electrochemical characteristics of a carbon fibre composite and the associated galvanic effects with aluminium alloys. Applied Surface Science 2014;314:233–40.

[46] Srinivasan R, Nelson JA, Hihara LH. Development of guidelines to attenuate galvanic corrosion between mechanically-coupled aluminum and carbon-fiber reinforced epoxy composites using insulation layers. Journal of The Electrochemical Society 2015;162:C545–54.

[47] Zou S, Zhang Y, Xu W, Wan Y, He C, Dong C, et al. Galvanic Corrosion Behavior of Aluminum Alloy (2219 and ZL205A) Coupled to Carbon Fiber-Reinforced Epoxy Composites. INTERNATIONAL JOURNAL OF ELECTROCHEMICAL SCIENCE 2016;11:9625–33.

[48] Polmear I, StJohn D, Nie J-F, Qian M. Light alloys: metallurgy of the light metals. Butterworth-Heinemann; 2017.

[49] Ryen Ø, Holmedal B, Nijs O, Nes E, Sjölander E, Ekström H-E. Strengthening mechanisms in solid solution aluminum alloys. Metallurgical and Materials Transactions A 2006;37:1999–2006.

[50] Jiang H, Ye L, Zhang X, Gang GU, Zhang P, Wu Y. Intermetallic phase evolution of 5059 aluminum alloy during homogenization. Transactions of Nonferrous Metals Society of China 2013;23:3553–60.

[51] Radetić T, Popović M, Romhanji E. Microstructure evolution of a modified AA5083 aluminum alloy during a multistage homogenization treatment. Materials Characterization 2012;65:16–27.

[52] Leo P, D'Ostuni S, Casalino G. Hybrid welding of AA5754 annealed alloy: Role of post weld heat treatment on microstructure and mechanical properties. Materials & Design 2016;90:777–86.

[53] Lambiase F, Genna S, Leone C, Paoletti A. Laser-assisted direct-joining of carbon fibre reinforced plastic with thermosetting matrix to polycarbonate sheets. Optics & Laser Technology 2017;94:45–58.

[54] Halambek J, Berković K, Vorkapić-Furač J. Laurus nobilis L. oil as green corrosion inhibitor for aluminium and AA5754 aluminium alloy in 3% NaCl solution. Materials Chemistry and Physics 2013;137:788–95.

[55] Davó B, De Damborenea JJ. Use of rare earth salts as electrochemical corrosion inhibitors for an Al–Li–Cu (8090) alloy in 3.56% NaCl. Electrochimica Acta 2004;49:4957–65.

[56] Songür M, Çelikkan H, Gökmeşe F, Şimşek SA, Altun NŞ, Aksu ML. Electrochemical corrosion properties of metal alloys used in orthopaedic implants. Journal of Applied Electrochemistry 2009;39:1259.

[57] Zhang Z, Shan J-G, Tan X-H, Zhang J. Effect of anodizing pretreatment on laser joining CFRP to aluminum alloy A6061. International Journal of Adhesion and Adhesives 2016;70:142–51.

Joint	Technology	Mechanical characterization	Morphological characterization	Electrochemical characterization
CF/epoxy- PA6-AA5754	Ultrasonic spot welding	Lap-shear test	Optical microscopy SEM-EDS	Potentiostatic Potentiodynamic ZRA
CF/epoxy – PA6-CF/epoxy	Adhesive bonding	Lap-shear test	-	-
AA5754-PA6-AA5754	Adhesive bonding	Lap-shear test	-	-

Table 1 Analyzed joint typologies and experimental plan.

Material	E_{corr} V vsAg/AgCl	i_{corr} µA cm^{-2}	E_{pit} V vsAg/AgCl
AA5754	-0.759	2.87	-0.676
CFRP	-0.205	1.13	
Welded hybrid joint	-0.757	2.64	-0.671

Table 2 – Corrosion potential, corrosion current density and pitting potential extracted from potentiodynamic polarization curves reported in Figure 9b.

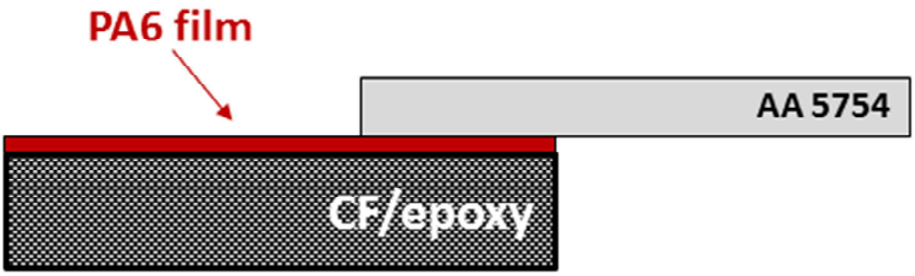

Figure 1 Sketch (not in scale) of the hybrid CF/epoxy-Aluminum joint

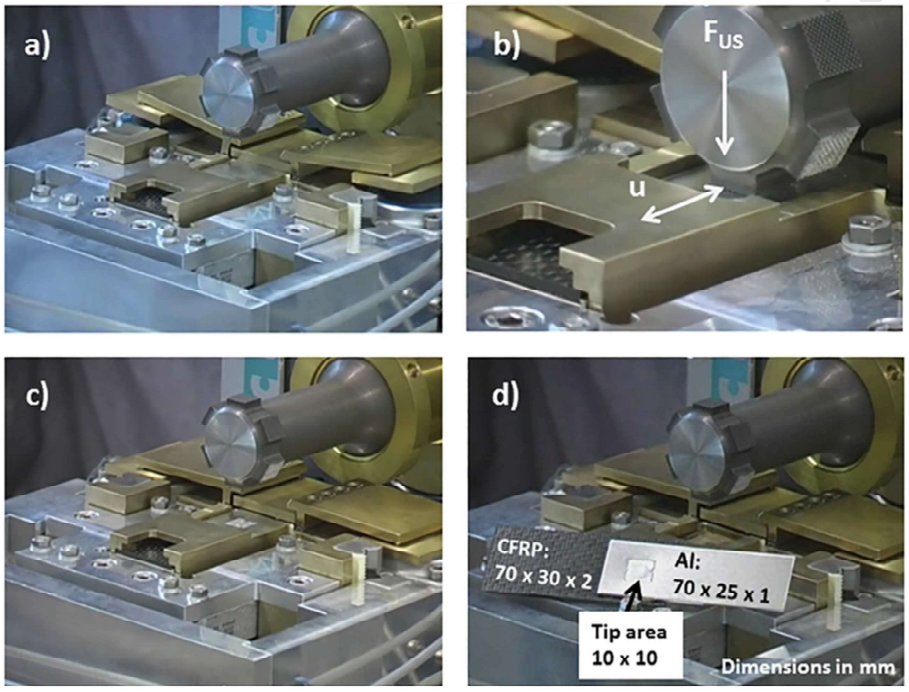

Figure 2 Experimental setup for ultrasonic metal welding: a) composite-aluminum joint loaded in the clamping system; b) sonotrode tip at contact with the aluminum adherend during ultrasonic spot welding; c) raised sonotrode and disabled clamping tools; d) CF/epoxy-AA5754 joint after ultrasonic welding.

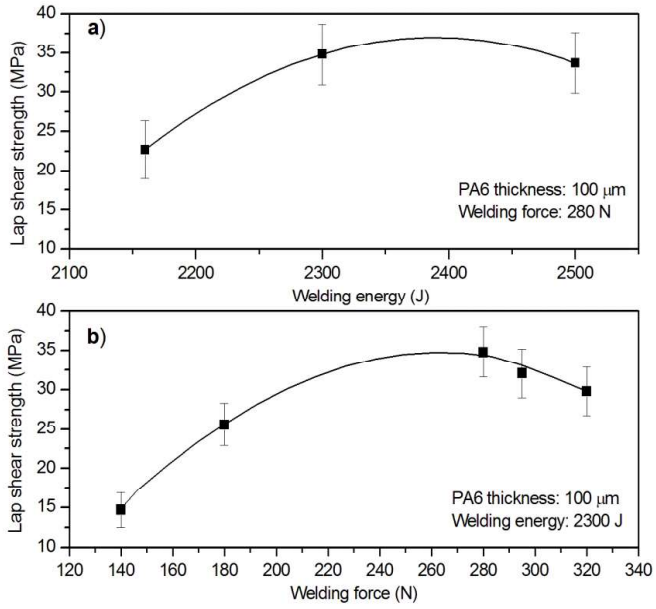

Figure 3 Effect of welding energy (a) and welding force (b) on the tensile shear strength of CF/epoxy-Aluminum joints with a PA6 thickness of 100 µm with a constant oscillation amplitude of 40 µm.

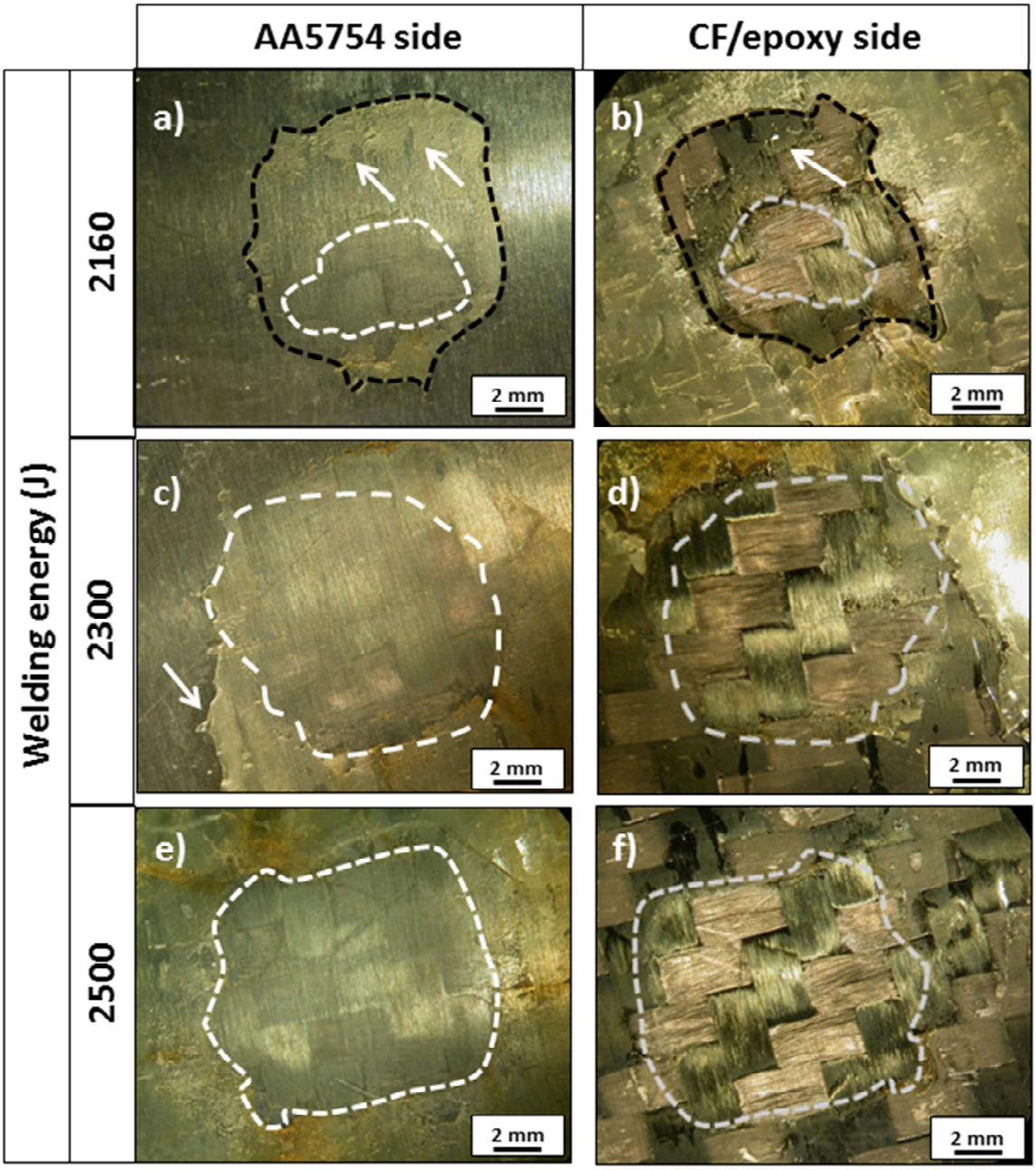

Figure 4 Fracture surfaces of hybrid Al/CF-epoxy joints welded at different welding energy and a constant welding force of 280 N (A: adhesion zone; I: mechanical interlocking zone).

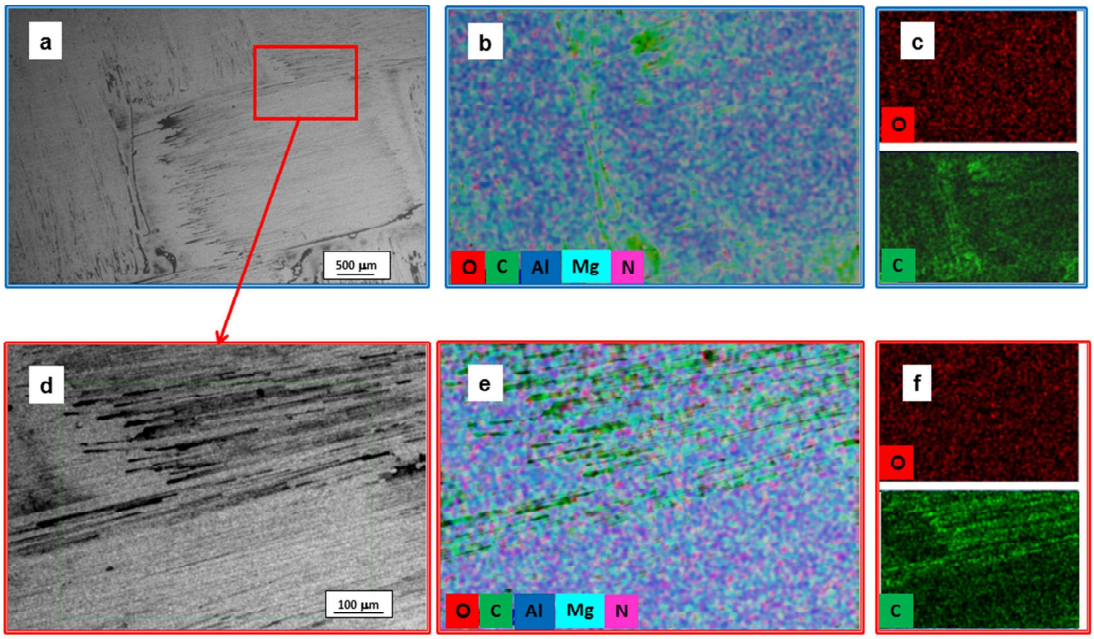

Figure 5 SEM/EDS-analysis of aluminum side of fracture surfaces.

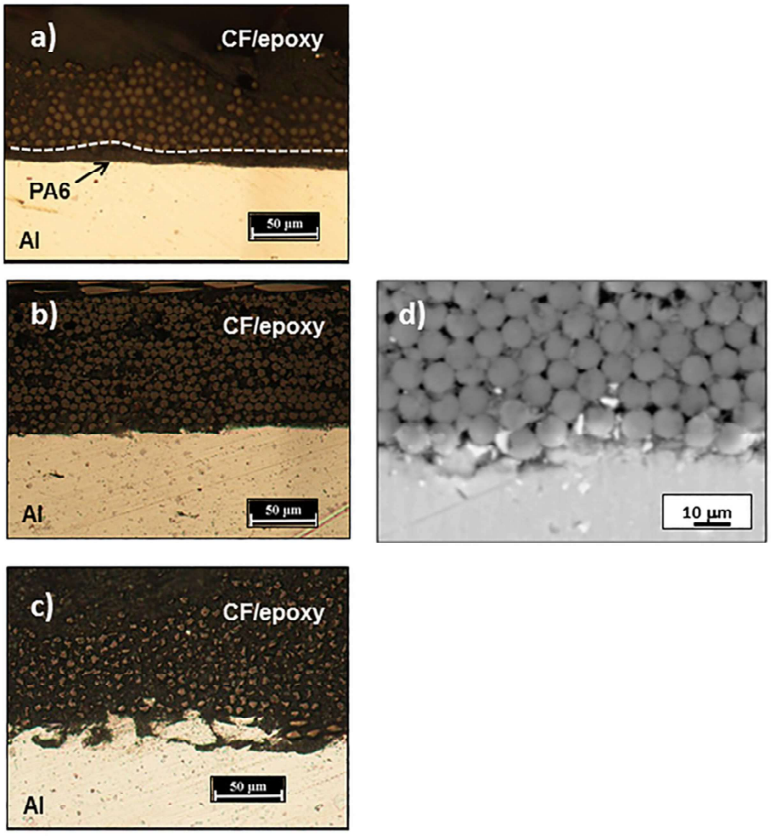

Figure 6 Optical micrographs of cross-sections of CF/epoxy-AA5754joints after ultrasonic metal welding with 40 µm oscillation amplitude and 280 N welding force and 2160 J (a), 2300 J (b) and 2500 J (c) welding energy; d) SEM image of hybrid joint welded at 2300 J.

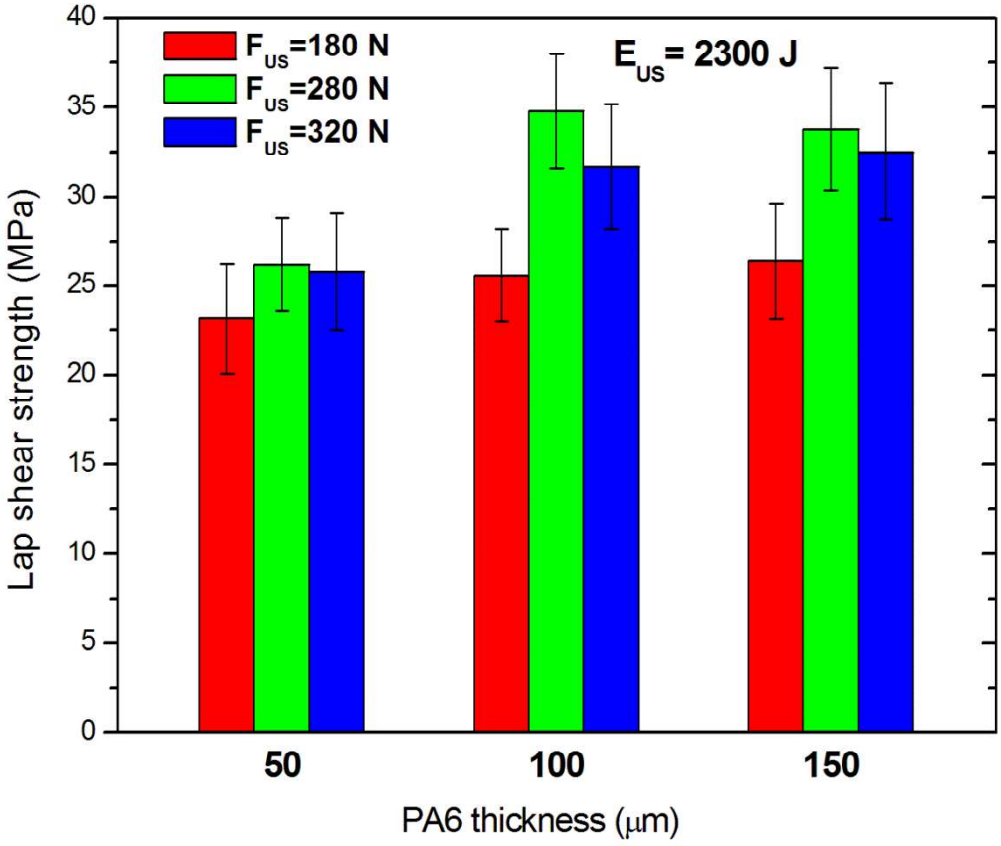

Figure 7 Effect of PA6 film thickness and ultrasonic welding force on tensile shear strength of hybrid joints ultrasonically welded with a welding energy of 2300 J.

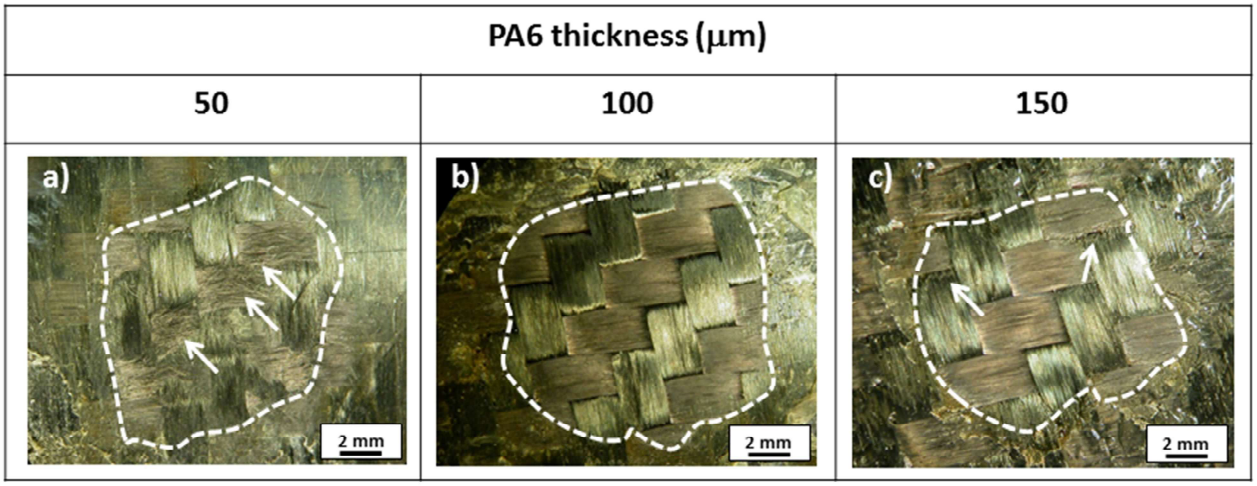

Figure 8 Fracture surfaces of CF-epoxy-AA5754 joints with different thickness of PA6 film.

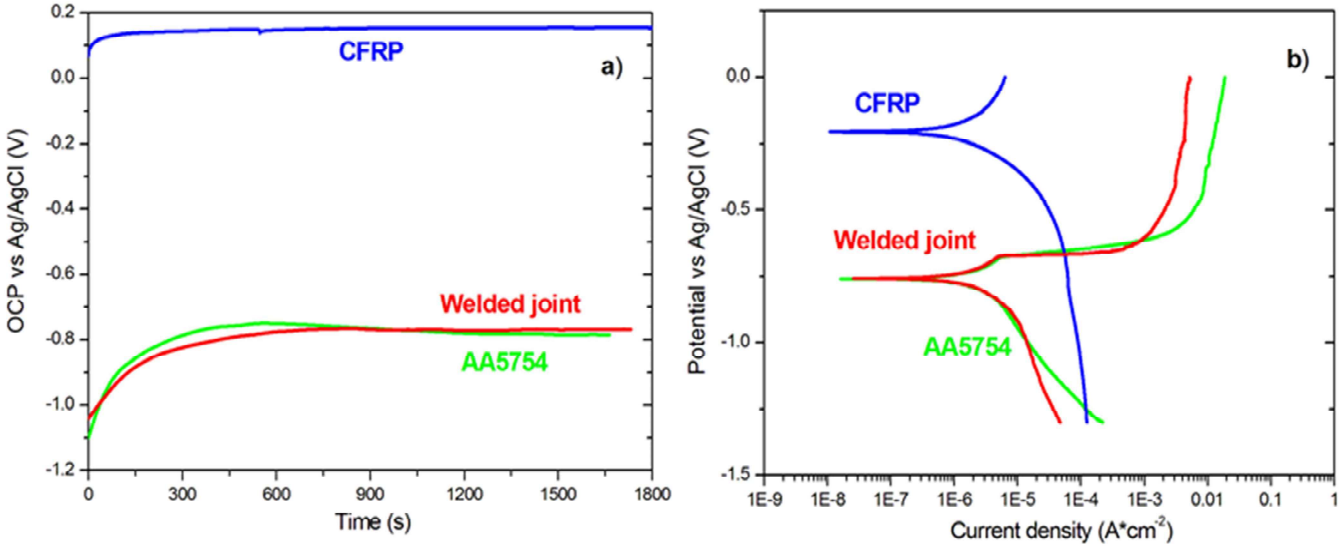

Figure 9 – (a) Open circuit potential and (b) potentiodynamic polarization curves of AA5754, CFRP and welded hybrid joint tested in 3.5% NaCl solution.

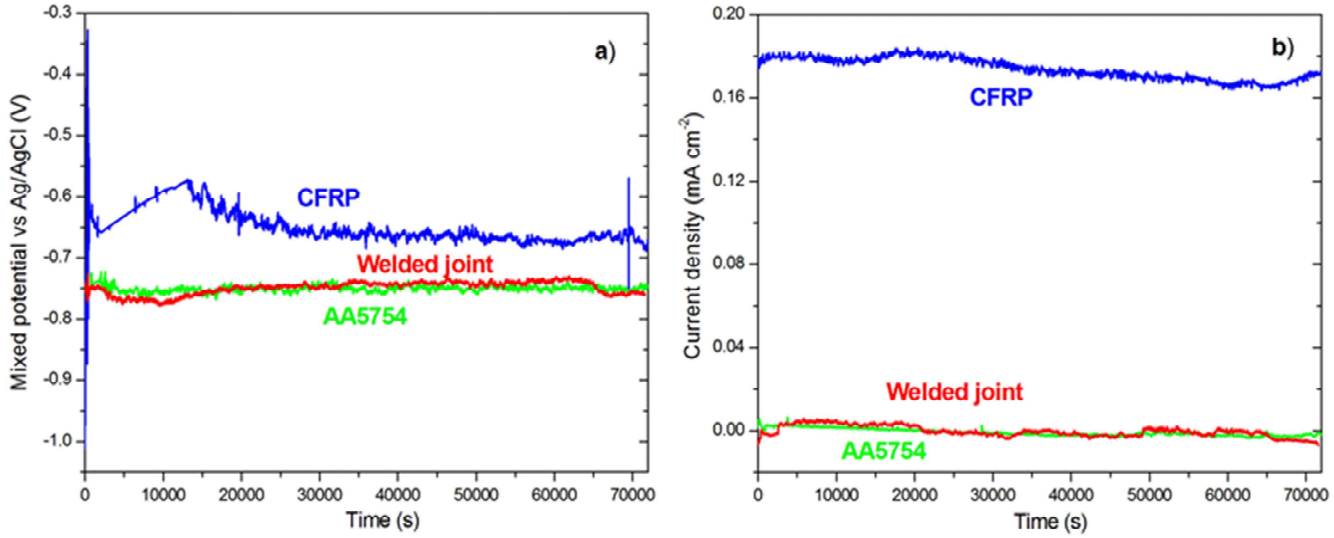

Figure 10 – (a) Mixed corrosion potential and (b) galvanic current density of AA5754, CFRP and welded hybrid joint obtained by ZRA galvanic corrosion tests in 3.5% NaCl solution.